



Citation for published version:

Guy, RH & Szoka, FC 2011, 'Perturbation of solute transport at a liquid-liquid interface by polyethylene glycol (PEG): implications for PEG-induced biomembrane fusion', *Physical Chemistry Chemical Physics*, vol. 13, no. 12, pp. 5346-5352. <https://doi.org/10.1039/c0cp02305a>

DOI:

[10.1039/c0cp02305a](https://doi.org/10.1039/c0cp02305a)

Publication date:

2011

[Link to publication](#)

Reproduced by permission of the PCCP Owner Societies

University of Bath

General rights

Copyright and moral rights for the publications made accessible in the public portal are retained by the authors and/or other copyright owners and it is a condition of accessing publications that users recognise and abide by the legal requirements associated with these rights.

Take down policy

If you believe that this document breaches copyright please contact us providing details, and we will remove access to the work immediately and investigate your claim.

**PERTURBATION OF SOLUTE TRANSPORT AT A LIQUID-LIQUID INTERFACE BY POLYETHYLENE
GLYCOL (PEG): IMPLICATIONS FOR PEG-INDUCED BIOMEMBRANE FUSION**

Richard H. Guy^{a,b} and Francis C. Szoka, Jr.^b

^aDepartment of Pharmacy & Pharmacology

University of Bath

Claverton Down

Bath, BA2 4LZ; U.K.

r.h.guy@bath.ac.uk; +44.1225.384901 (tel.); +44.1225.386114 (fax)

^bDepartments of Bioengineering & Therapeutic Sciences and Pharmaceutical Chemistry

School of Pharmacy

University of California, San Francisco

San Francisco, CA 94143-0912, U.S.A.

ABSTRACT

The effect of polyethylene glycol 400 (PEG) dissolved at various concentrations (0-40% v/v) in water, on the interfacial transport of methyl nicotinate across an aqueous - isopropyl myristate interface was investigated with a rotating diffusion cell. At four temperatures studied (20-37°C), the presence of PEG decreased the rate of solute transfer both into and out of the organic phase in a concentration-dependent fashion. The bulk partition coefficient of the solute (organic/aqueous) increased with increasing PEG in the aqueous phase. Analysis of the temperature dependence of the interfacial transfer kinetics allowed thermodynamic activation energy parameters for the phase transport process to be determined. Although the free energy of activation (ΔG^\ddagger) for transfer was not affected by PEG, the relative enthalpic and entropic contributions were dramatically altered. At PEG concentrations of 10-40% v/v, the enthalpic portion of ΔG^\ddagger was decreased by about a factor of two, while the entropic contribution (which is large and positively favorable in the absence of PEG) was reduced considerably such that it was totally eliminated at higher PEG levels. These observations suggest novel and direct experimental evidence for the concept that high PEG concentrations substantially alter water structure at an aqueous solution – organic liquid biomembrane model interface. The results support the hypothesis that the critically important function of PEG in inducing cell-cell and liposome-liposome fusion is to remove the hydration layer that impedes the close apposition of converging phospholipid bilayers.

Key Words:

Cell fusion; interfacial transfer kinetics; model membranes; membrane transport; polyethylene glycol

INTRODUCTION

Techniques to fuse cells, which have led to important advances in somatic cell genetics^{1,2}, reconstitution of receptor complexes⁴ or for the delivery of exogenous macromolecules into cells^{5,6}, have depended upon the ability of polyethylene glycol (PEG) solutions to mediate the fusion process. This widespread use has outstripped our understanding of how these solutions work. Fusogenic concentrations of PEG (50% w/v) bind essentially all of the free water in solution⁷⁻⁹ and this has provoked the suggestion that PEG induces fusion by altering or removing the hydration layer from the head group region of the phospholipids⁸. Polyethylene glycol also brings about a marked decrease in the surface potential of both phosphatidylcholine and phosphatidylethanolamine monolayers¹⁰.

In phospholipid bilayer systems, PEG solutions (50% w/v) cause an increase in the transition temperature of synthetic phosphatidylcholine and phosphatidylethanolamine altering the cooperativity, enthalpy, and entropy of transitions⁹. In phospholipid dispersions, low concentrations of PEG cause aggregation^{9,11} whereas, at higher levels (40-50% w/v), PEG mediates a rearrangement of sonicated unilamellar vesicles to the multilamellar structures, and this has been suggested to be a fusion phenomenon¹¹. Freeze-fracture studies have revealed that fusogenic concentrations of PEG induce structural defects in phosphatidylcholine bilayers and the appearance of a non-bilayer phase¹¹. The appearance of non-bilayer structures was not observed when glycerol or dextran at similar concentrations, which are known to dehydrate the lipids, were used¹². Arnold¹³ has proposed that the major effect of PEG is a volume-exclusion induced aggregation and dehydration of the bilayer interface and this hypothesis has garnered considerable biophysical support from Lentz and others¹⁴.

In this report, the influence of fusogenic concentrations of PEG on the interfacial transfer kinetics of methyl nicotinate across isopropyl myristate impregnated membranes in a rotating diffusion cell¹⁵ is examined. This system permits investigations into the kinetic and thermodynamic properties of interfacial transport. The data indicate to us that, in the presence of fusogenic concentrations of PEG, the hydration layer at the interfacial region of the two-phase, aqueous solution-organic liquid system is greatly diminished which is consistent with results obtained using other experimental techniques¹⁴.

MATERIALS & METHODS

Interfacial transfer kinetics were studied with a rotating diffusion cell (RDC), which has been described elsewhere¹⁵. Essentially, an organic liquid-impregnated Millipore filter (GS type, 0.22 μm size, Millipore Corp., Billerica, MA) separates an aqueous donor solution of transferring substrate from an aqueous receptor phase. Liquid-liquid interfaces are thus established on both surfaces of the filter, the area of which, corrected for porosity, defines the interfacial area. Transport to and from the interfacial regions is controlled by rotating disc hydrodynamics, which are produced by the design and rotation of the diffusion cell as previously discussed^{15,16}.

Elucidation of the interfacial perturbations induced by polyethylene glycol 400 (PEG, approximate molecular weight = 400 Daltons) (Sigma Chemical Co., St. Louis) involved monitoring the transport of a model solute in the RDC as a function of temperature (T). Experimental systems of four different initial configurations were studied, the details of which are summarized in Table I.

Methyl nicotinate (3-pyridine carboxylic acid methyl ester, MN) (Sigma) was selected as the transferring substrate because its frequent use in earlier RDC work has made available a number of its physical properties which are essential for data interpretation. Furthermore, the solute's high aqueous solubility, which allowed a steep concentration gradient to be initially developed across the organic liquid-filled filter, enabled improved precision in the results. The solute flux was assayed by periodic sampling and UV spectrophotometric analysis of the aqueous receptor phase solution.

The organic lipid, isopropyl myristate (IPM) (Sigma), with which the RDC filter was impregnated, was chosen for its ability to simulate certain properties of biomembrane structure. IPM has been used frequently^{15,17} in drug absorption and distribution studies to mimic various membrane lipids and it allows attention to be focused on the properties of the hydration layer while minimizing the interaction of PEG with the amphiphilic portion of the membrane.

As seen in Table I, transport experiments (A-D) across the organic liquid barrier were performed with and without PEG 400 in the aqueous donor and receptor phases. Three PEG 400 concentrations (40% 25%, and 10% v/v) were studied. Additionally, important control experiments were performed as part of this investigation:

1. A sample of the commercial PEG employed was purified by ether precipitation and RDC experiments were then conducted using aqueous solutions prepared with the extracted polymer.

2. The thickness of the rotating membrane was doubled by collapsing together two Millipore filters during the cell preparation process. The dual membrane was then impregnated with IPM in the normal way before measuring solute permeation as described above.
3. A series of transport experiments were carried out in which the 40% PEG solutions were replaced by 40% glycerol. All other aspects of the transport measurement procedure remained unaltered.

The initial experimental configurations of the three controls (C1, C2, C3) are also summarized in Table I; their respective rationales were as follows:

- (a) An early report suggested that organic solvent-soluble impurities in the commercially available PEG are responsible for the fusogenic properties of the hydrophilic polymer¹⁸. Although a later study¹⁹ has suggested that this is not the case for the PEG used in our work, it was nevertheless desirable to check that the purified polymer behaved similarly under the conditions of the experiments performed.
- (b) In the data reduction to obtain interfacial transfer kinetics from an RDC experiment, it is necessary to subtract the membrane diffusion resistance from the total permeation barrier (see below). In the second control, we maintain hydrodynamic and interfacial barriers constant and change the membrane (IPM – impregnated filter) resistance in a pre-determined manner. It is possible, in this way, to demonstrate unequivocally the correct assignment of the transport resistance to the various contributing barriers established in RDC.
- (c) Glycerol, like PEG, is a viscous hydrophilic moiety of high water solubility but it does not induce bilayer fusion when present at concentrations at which PEG is fusogenic. To ensure that any RDC-detected effects of PEG were likewise distinct from those of glycerol, the third control was deemed a necessary aspect of this work.

Analysis of all experimental results including controls (see Theory below) required, at each temperature studied, knowledge of (i) the substrate organic liquid/aqueous phase partition coefficients, and (ii) the diffusion coefficients of the solute in IPM. The former were found classically as reported in earlier publications¹⁵; the latter were available in the literature¹⁵.

THEORY

The rate of transfer (J mol·s⁻¹) of substrate from the donor compartment of the RDC to the receptor is given by an equation analogous to Fick's 1st Law of Diffusion:

$$J = A \cdot P \cdot (C_D - C_R) \quad (1)$$

where A is the area of the filter across which transport occurs and C_D and C_R are the solute concentrations in the aqueous donor and receptor phases, respectively. P is the overall effective permeability coefficient for the substrate and is associated with three distinct resistances to movement across the rotating filter¹⁵, i.e.:

$$\frac{1}{P} = \frac{2 \cdot z_D}{D_a} + \frac{L}{\alpha \cdot K \cdot D_o} + \frac{2}{\alpha \cdot k_{ao}} \quad (2)$$

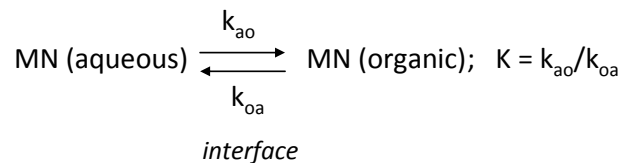
$2 \cdot z_D / D_a$ is the barrier to solute transport caused by stagnant diffusion layers in the aqueous phases on either side of the organic liquid-filled filter. This hydrodynamic resistance is the result of the cell rotation and the thickness of the boundary layers (z_D) is given by the Levich equation²⁰:

$$z_D = 0.643 \cdot \nu^{1/6} \cdot D_a^{1/3} \cdot \omega^{-1/2} \quad (3)$$

where ν is the kinematic viscosity of the aqueous solvent, D_a is the substrate aqueous phase diffusion coefficient and ω (revolutions per second) is the rotation speed of the filter.

$L / \alpha \cdot K \cdot D_o$ is the diffusional resistance (R_M) offered to solute movement by the organic liquid-filled filter of length L and porosity α . K is the solute's organic/aqueous partition coefficient and D_o its diffusion coefficient in the organic liquid.

$2 / \alpha \cdot k_{ao}$ corresponds to the interfacial resistance (R_i), i.e., the barrier to solute transport across the two interfacial regions between the aqueous phase and the organic liquid. Schematically, one may represent interfacial transfer rate constants k_{ao} and k_{oa} as follows:



and hence one may recognize that $2 / \alpha \cdot k_{ao}$ is merely shorthand for two terms ($1 / \alpha \cdot k_{ao} + 1 / \alpha \cdot K \cdot k_{oa}$) that more obviously relate to the two interfacial transfer processes which take place during the movement of a solute molecule from the donor compartment of the RDC to the receptor.

Combination of Eqs. (2) and (3) shows that measurement of P^{-1} as a function of rotation speed enables evaluation of the sum $L/\alpha \cdot K \cdot D_o + 2/\alpha \cdot k_{ao}$. Knowledge of the first of these terms then allows determination of the interfacial transfer rate constants k_{ao} and k_{oa} (since $k_{ao} = K \cdot k_{oa}$).

The activation free energy barriers associated with the kinetic parameters can be obtained using Eq. (4)¹⁵:

$$\Delta G_i^\ddagger = R \cdot T \cdot \ln(k_i / Z) \quad (4)$$

(where the subscript i replaces either ao or oa). In this equation, a frequency factor Z of $100 \text{ m}\cdot\text{s}^{-1}$ is included²¹.

Finally, the temperature dependence of the transport process generates further thermodynamic information. The slope of an Arrhenius-type plot of $\ln k_i$ against reciprocal absolute temperature ($1/T$) gives ΔH_i^\ddagger the enthalpic contribution to the free energy barrier, and subsequently ΔS_i^\ddagger , the entropy, is found by difference:

$$\Delta S_i^\ddagger = (\Delta H_i^\ddagger - \Delta G_i^\ddagger) / T \quad (5)$$

The substrate's bulk partition coefficient (K) and its variation with T can be utilized in a similar fashion to obtain corresponding information for bulk, rather than interfacial, transfer²².

RESULTS

Methyl nicotinate flux measurements were performed in the RDC as a function of rotation speed, temperature and PEG concentration as shown in Table I. A typical set of experimental data for a PEG concentration of 40% v/v is shown in Figure 1. Regression lines through the results have been drawn to derive intercepts on the P^{-1} axis at $\omega^{-1/2} = 0$. Here the resistance of the stagnant diffusion layers is zero and the value of P^{-1} is the sum of membrane diffusional and interfacial transport barriers ($L/\alpha \cdot K \cdot D_o + 2/\alpha \cdot k_{oa}$). The relative contribution of these two terms may be found because the first resistance is calculable from known parameters. In Table II, the partition coefficient (K) values determined in this study are presented for the various systems together with the corresponding methyl nicotinate diffusion coefficient (D_o) in IPM which has been reported elsewhere¹⁵.

The possibility that in our experiments, PEG partitions into IPM and alters its solvent characteristics (and hence D_o for a solute diffusing through it), was checked by attempting to distribute radiolabeled PEG between water and the organic liquid. No radioactivity above background was ever found in the IPM. The characteristics, L and α , are given by Millipore as 150 μm and 0.75, respectively. These values have been independently verified using an elegant electrochemical technique²³.

Thus, the experimentally determined intercepts of plots of P^{-1} versus $\omega^{-1/2}$ provide the transport resistances and contributions. In Table III, the intercept values found are given and the relative contributions due to membrane and interfacial barriers (R_M and R_i , respectively) are calculated. Also given in this Table are the regression slopes through the individual data sets. In accord with theory (Eqs. (2) and (3)), the gradients increase with increasing PEG in the aqueous phase and increase with decreasing temperature (reflecting, respectively, increasing viscosity (ν) and decreasing diffusion coefficient (D_o)). From the interfacial resistance and the partition coefficients, the phase transfer rate constants k_{oa} and k_{oo} can be found for each system and temperature studied. These kinetic parameters are displayed graphically as a function of PEG concentration employed in Figure 2.

The free energies of activation (ΔG_i^\ddagger) associated with the interfacial transfer rate constants were determined using Eq. (4) and the values are given in Table IV. Enthalpic and entropic contributions to ΔG_i^\ddagger , derived at 25°C as described in the Theory, are presented in Figure 3, the former showing the thermodynamic parameters for the k_{oa} process, the latter the energetics associated with k_{oo} .

Finally, the temperature dependence of the bulk partition coefficients given in Table II is used to access the thermodynamic parameters at 25°C associated with solute movement from the bulk aqueous

phase to the bulk organic phase. These energetics at each PEG concentrations in the aqueous phase are summarized in Table V.

Control experiments

1. Purified PEG: Using extracted polymer and experimental configuration C1 shown in Table I, methyl nicotinate flux at 25°C was measured at two rotation speeds. It was found that $P^{-1} = 4.24 \times 10^5 \text{ m}^{-1}\cdot\text{s}$ at 494 rpm ($\omega^{-1/2} = 0.622 \text{ s}^{1/2}$) and $P^{-1} = 4.84 \times 10^5 \text{ m}^{-1}\cdot\text{s}$ at 298 rpm ($\omega^{-1/2} = 0.449 \text{ s}^{1/2}$). These values did not differ significantly from those observed when unpurified PEG was employed.

2. Membrane diffusion resistance: This control involved measurement of solute transport across a double thickness IPM-impregnated filter paper barrier (configuration C2, Table I). Nicotinate flux was monitored at three rotation speeds (319, 341 and 367 rpm) and the results were extrapolated in the normal way to yield an intercept of $7.34 (\pm 0.27) \times 10^5 \text{ m}^{-1}\cdot\text{s}$. The single membrane barrier gave an intercept of $3.41 \times 10^5 \text{ m}^{-1}\cdot\text{s}$ and an interfacial resistance ($R_i = 2/\alpha \cdot k_{ao}$) of $1.09 \times 10^5 \text{ m}^{-1}\cdot\text{s}$. From these individuals resistance, we can theoretically calculate the resistance of the double membrane. First, α must change because the filter pores will overlap in a random fashion, thereby reducing the effective porosity. Assuming that there is random distribution of pores then the effective porosity of the double filter must be α^2 or 0.56. Secondly, for the connecting pores L will double in length to 300 μm . Thus, from the single filter resistances we may calculate R_M and R_i for the double membrane to be $6.19 \times 10^5 \text{ m}^{-1}\cdot\text{s}$ and $1.45 \times 10^5 \text{ m}^{-1}\cdot\text{s}$, respectively. The sum is the predicated intercept, $7.64 \times 10^5 \text{ m}^{-1}\cdot\text{s}$, which is not distinguishable from the experimental value.

3. Glycerol Experiment: To check that the effect of PEG on methyl nicotinate interfacial transfer was distinct from that of glycerol, the controls designated C3 in Table I were conducted. Three rotation speeds at each temperature were studied. 40% v/v glycerol solution viscosities were measured with an Ostwald viscometer at both temperatures so that theoretical RDC gradients were known. Solute partition coefficients were determined in the unusual way to allow appropriate evaluation of the membrane resistance contribution to P^{-1} . From the intercepts, thus, interfacial transfer rate constants were evaluated. These are given in Table VI and are compared to those obtained when the inner and outer compartment phases were water. Agreement is very good and the values differ markedly from those found when 40% v/v PEG is the aqueous medium. We deduce that glycerol (at 40% v/v) has minimal effects on the nicotinate transport in this system compared to PEG.

DISCUSSION

The transport resistance and contribution data in Table III show that phase transfer kinetics play a key role in the systems studied and confirm the utility of this process as a probe for interfacial events. The rate constants for interfacial transfer decrease as the % PEG used in these experiments increases (see Figure 2). The change is reflected by the increase in transport resistance due to the phase transfer process (Table III). Although it cannot be shown unequivocally from this data, the implication of the values in Figure 2 is that some PEG molecules may be populating the water - IPM interface thereby hindering solute movement in both directions (aqueous \rightarrow organic and organic \rightarrow aqueous). Our inability to identify any PEG partitioning into the organic phase suggest that, if PEG is present at the interface, it is localized on the aqueous side and has its action there.

The alteration of k_{oo} and k_{oa} by increasing amounts of PEG is also reflected in the bulk partition coefficients which have been determined in this study (see Table II). In the absence of PEG, increasing temperature leads to a disfavoring of the aqueous phase by the solute and subsequent rise in K . With increasing amount of PEG, however, this temperature dependence is gradually reversed such that, at 40% PEG, K decreases as the temperature rises. The thermodynamic data in Table V suggest some clues as to the reasons behind these observations. Firstly, the free energy (ΔG_K) for the process is weakly favorable in all cases (since K always exceeds unity). Secondly, as the percent PEG increases, ΔH_K switches from an endothermic to an exothermic value. This may suggest that the greater the percent PEG in the aqueous phase, the less efficient is solvation of the solute in water. Thirdly, as the percent PEG in water is decreased from 40% to zero, the entropy (ΔS_K) of solute movement from the bulk aqueous phase to the bulk organic phase becomes increasingly positive. This is consistent with the solute solvation efficiency indicated by ΔH_K . With no PEG present, it appears that bulk transfer of methyl nicotinate out of water is entropically favorable (due to the release of a solvation sphere of water, perhaps). At high PEG concentrations, though, we would expect little free water available and that solvating molecules released by the solute on transfer may be immediately restructured by the polymer. What the sequence of events taking place, it is clear that equilibrium substrate - PEG - water - IPM interactions are complex and require further study.

The thermodynamics associated with the interfacial transfer processes are now considered. It is first apparent that the activation free energy barrier to phase transport at the liquid-liquid interfaces studied is about 40 KJ mol⁻¹ (see Table IV). The values are consistent with previous determinations¹⁵ and insensitive to the concentration of PEG in the aqueous phase. Conversely, the enthalpic (ΔH^\ddagger) and

entropic (ΔS^\ddagger) contributions to ΔG^\ddagger are very dependent upon the presence of PEG (see Figure 3). When the aqueous phase is simply water, ΔG^\ddagger is the result of a large positive ΔH^\ddagger (for both k_{ao} and k_{oa} processes). The entropic term, however, acts so as to reduce the activation free energy barrier and is large and positive (159 J mol⁻¹K⁻¹ for k_{ao} , 121 J mol⁻¹K⁻¹ for k_{oa}). Because there is increasing disorder for solute transfer in both directions, the ΔS^\ddagger values have been interpreted²² as reflecting disruption of interfacial water structure by transferring substrate molecules. Such a hypothesis is consistent with a positive ΔS^\ddagger for both k_{ao} and k_{oa} processes. With PEG present in the aqueous phase, enthalpic and entropic contributions to ΔG^\ddagger (k_{ao} and k_{oa}) changed markedly. There appears a slight PEG concentration dependence but the gross effects are similar at all PEG levels studied. Firstly, ΔH^\ddagger is reduced by about a factor of two. However, this change is counteracted by the almost complete elimination of ΔS^\ddagger which, for all intents and purposes, goes to zero. In other words, the favorable ΔS^\ddagger , observed for methyl nicotinate crossing a simple water-IPM interface, is destroyed by the presence of PEG (at $\geq 10\%$ v/v) in the aqueous phase.

In conclusion, these observations, therefore, seem consistent with the thesis that PEG substantially reduces water structure at the aqueous solution - organic liquid interface. In terms of a putative mechanism by which PEG induces cell-cell fusion, the results of this investigation suggest new and direct evidence for the theory of hydration layer removal/destabilization and consequential allowed close approach of converging membranes^{8,9,11,13,14}. That is, this study provides additional evidence for the mechanism of PEG induced bilayer aggregation and fusion put forward 25 years ago by Arnold *et al.*^{13,14}

ACKNOWLEDGEMENTS

This research was partially supported in part by a grant (R01-EB0003008) from the U.S. National Institutes of Health (FCS). We thank Robert Hinz, in particular, and Tim Aquino, Don Honda, Britt Kaufman, Diane Milholland, Susan Stanlis, and Michael Amantea for their experimental assistance, and Professor W. John Albery, FRS, for his inspiration and insight.

REFERENCES

- 1 G. Pontecorvo. Production of mammalian somatic cell hybrids by means of polyethylene glycol treatment. *Somatic Cell Genet.*, 1975, **1**, 397-400.
- 2 R.L. Davidson, K.A. O'Malley and T.B. Wheeler. Polyethylene glycol-induced mammalian cell hybridization: effect of polyethylene glycol molecular weight and concentration. *Somatic Cell Genet.*, 1976, **2**, 271-280.
- 3 K.N. Kao and M.R. Kichayluk. A method for high-frequency intergeneric fusion of plant protoplasts. *Planta*, 1974, **115**, 355-367.
- 4 D. Doyle, E. Hou and R. Warren. Transfer of the hepatocyte receptor for serum asialoglycoproteins to the plasma membrane of a fibroblast. Acquisition of the hepatocyte receptor functions by mouse L-cells. *J. Biol. Chem.*, 1979, **254**, 6853-6856.
- 5 R.A. Schlegel and M.C. Rechsteiner. Red cell-mediated microinjection of macromolecules into mammalian cells. *Methods Cell Biol.*, 1978, **20**, 341-354.
- 6 F. Szoka, K.E. Magnusson, J. Wojcieszyn, Y. Hou, Z. Derzko and K. Jacobson. Use of lectins and polyethylene glycol for fusion of glycolipid-containing liposomes with eukaryotic cells. *Proc. Natl. Acad. Sci. U S A.*, 1981, **78**, 1685-1689.
- 7 A.A. Baran, I.M. Solomentseva, V.V. Mank and O.D. Kurilenko. 1972. Role of the solvation factor in stabilizing disperse systems containing water-soluble polymers. *Dokl. Akad. Nauk SSSR*, 1972, **207**,: 363-366.
- 8 A.M.J. Blow, G.M. Bothan, D. Fisher, A.H. Goodall, C.P.S. Tilcock and J.A. Lucy. Water and calcium ions in cell fusion induced by poly (ethylene glycol). *FEBS Lett.*, 1978, **94**, 305-310.
- 9 C.P. Tilcock and D. Fisher. Interaction of phospholipid membranes with poly(ethylene glycol)s. *Biochim. Biophys. Acta*, 1979, **557**, 53-61.
- 10 B. Maggio, Q.F. Ahkong and J.A. Lucy. Poly(ethylene glycol), surface potential and cell fusion. *Biochem. J.*, 1976, **158**, 647-650.
- 11 L.T. Boni, T.P. Stewart, J.L. Alderfer and S.W. Hui. Lipid-polyethylene glycol interactions: I. Induction of fusion between liposomes. *J. Memb. Biol.*, 1981a, **62**, 65-70.
- 12 L.T. Boni, T.P. Stewart, J.L. Alderfer and S.W. Hui. Lipid-polyethylene glycol interactions: II. Formation of defects in bilayers. *J. Memb. Biol.*, 1981b, **62**, 71-77.
- 13 K. Arnold, A. Herrmann, K. Gawrisch and L. Pratsch. Mechanism of poly(ethylene oxide)-induced fusion. *Stud. Biophys.* 1985. **110**, 135-141.
- 14 B.R. Lentz. PEG as a tool to gain insight into membrane fusion. *Eur. Biophys.J.*, 2007, **36**, 315-326.
- 15 W.J. Albery, J.F. Burke, E.B. Leffler and J. Hadgraft, J. Interfacial transfer studied with a rotating diffusion cell. *J. Chem. Soc. Faraday I*, 1976, **72**, 1618-1626.
- 16 W.J. Albery and J. Hadgraft. Percutaneous absorption: interfacial transfer kinetics. *J. Pharm. Pharmacol.*, 1979, **31**, 65-68.
- 17 J. Houk and R.H. Guy. Membrane models for skin penetration studies. *Chem. Rev.*, 1988, **88**, 455-471.
- 18 C.L. Smith, Q.F. Ahkong, D. Fisher and J.A. Lucy. Is purified poly(ethylene glycol) able to induce cell fusion? *Biochim Biophys Acta*, 1982, **692**, 109-114.

- 19 R.A. Parente and B. R. Lentz. Rate and extent of polyethylene glycol-induced large vesicle fusion monitored by bilayer and internal contents mixing. *Biochemistry*, 1986, **25**, 6678–6688.
- 20 V.G. Levich. *Physicochemical Hydrodynamics*. Prentice-Hall, Englewood Cliff, NJ, 1962, p. 69.
- 21 R.A. Marcus. On the theory of oxidation-reduction reactions involving electron transfer V. Comparison and properties of electrochemical and chemical rate constants. *J. Phys. Chem.*, 1963, **67**, 853-857.
- 22 R. Fleming, R.H. Guy and J. Hadgraft. Kinetics and thermodynamics of interfacial transfer. *J. Pharm. Sci.*, 1983, **72**, 142-145.
- 23 W.J. Albery, R.A. Choudery and P.R. Fisk. Kinetics and mechanism of interfacial reactions in the solvent extraction of copper. *Faraday Disc.*, 1984, **77**, 53-65.

Table I: Initial experimental configurations of the systems studied.

System	Aqueous donor phase (vol = 40 cm ³)	Organic liquid membrane	Aqueous receptor phase (vol = 250 cm ³)	T (°C)
A	0.1M MN ^a in water ^b	IPM ^a	Water	25,30,37
B	0.1M MN in 40% v/v PEG ^a	IPM	40% v/v PEG	20,25,30,37
C	0.1M MN in 25% v/v PEG	IPM	25% v/v PEG	20,25,30,37
D	0.1M MN in 10% v/v PEG	IPM	10% v/v PEG	20,30,37
C1	0.1M MN in 10% v/v PEG	IPM	10% v/v PEG	25
C2	0.1M MN in water	2 x IPM ^c	Water	25
C3	0.1M MN in 40% v/v glycerol	IPM	40% v/v glycerol	20,37

^aMN = methyl nicotinate; IPM = isopropyl myristate; PEG = polyethylene glycol 400.

^bAqueous solutions were prepared with water distilled from an all-glass apparatus.

^cA double-thickness membrane was used in this experiment.

Table II: Methyl nicotinate diffusion coefficients in IPM (D_o) and partition coefficients (K) between IPM and aqueous solutions containing increasing amounts (%v/v) of PEG.

T (°C)	$10^5 \cdot D_o$ (cm ² ·s ⁻¹)	K(IPM/aq)			
		aq = water	aq = 10% PEG	aq = 25% PEG	aq = 40% PEG
20	0.37	2.13	1.96	1.64	1.35
25	0.41	2.22	2.00	1.64	1.32
30	0.48	2.38	n.d.	1.61	1.28
37	0.51	2.59	2.22	1.61	1.23

Table III: Results from RDC experiments and transport resistances and contributions.

%PEG (v/v)	T (°C)	10^{-5} ·slope (m ⁻¹ ·s)	10^{-5} ·intercept (m ⁻¹ ·s)	R _M (%) ^a	R _I (%) ^b
40	20	4.60	7.30	57	43
	25	3.72	6.16	60	40
	30	3.12	5.34	65	35
	37	2.29	4.57	70	30
25	20	3.45	6.11	54	46
	25	2.84	5.07	59	41
	30	2.39	4.12	64	36
	37	1.85	3.63	67	33
10	20	2.30	4.43	62	38
	25	1.96	3.62	67	33
	37	1.38	2.36	75	25
5	25	1.37	3.41	68	32
	30	1.14	2.46	71	29
	37	1.97	1.84	83	17

$${}^a R_M = L/\alpha \cdot K \cdot D_o$$

$${}^b R_I = 2/\alpha \cdot k_{ao}$$

Table IV: Free energies of activation (ΔG_i^\ddagger) at 25°C associated with the kinetic parameters k_{ao} and k_{oa} for the systems studied.

% PEG (v/v)	$\Delta G_i^\ddagger, \text{aq} \rightarrow \text{org} \text{ (KJ}\cdot\text{mol}^{-1}\text{)}$	$\Delta G_i^\ddagger, \text{org} \rightarrow \text{aq} \text{ (KJ}\cdot\text{mol}^{-1}\text{)}$
40	40	40
25	41	39
10	40	38
0	40	38

Table V: Thermodynamic parameters at 25°C determined from the temperature dependence of the measured partition coefficients (reflecting the bulk transfer of solute from the aqueous to the organic phase).

Aqueous phase	40% v/v PEG	25% v/v PEG	10% v/v PEG	Water
$\Delta G_K \text{ (KJ}\cdot\text{mol}^{-1}\text{)}$	-0.7	-1.2	-1.7	-2.0
$\Delta H_K \text{ (KJ}\cdot\text{mol}^{-1}\text{)}$	-4.0	-0.9	+5.7	+9.1
$\Delta S_K \text{ (J}\cdot\text{mol}^{-1}\cdot\text{K}^{-1}\text{)}$	-11	+1	+25	+37

Table VI: Glycerol control experiments.

RDC aqueous phase	40% v/v glycerol		Water	
T (°C)	20	37 ^a	20	37
$10^6 \cdot k_{ao} \text{ (m}\cdot\text{s}^{-1}\text{)}$	19	61	21	86
$10^6 \cdot k_{oa} \text{ (m}\cdot\text{s}^{-1}\text{)}$	12	29	13	34

^aAlbery & Hadgraft¹⁶ report $k_{ao} = 66 \times 10^{-6} \text{ m}\cdot\text{s}^{-1}$ and $k_{oa} = 34 \times 10^{-6} \text{ m}\cdot\text{s}^{-1}$ for systems in which the aqueous phases were 60% v/v glycerol.

FIGURE LEGENDS

- Figure 1:** Dependence of total transport resistance (P^{-1}) on rotation speed (ω^{-2}) for System B (see Table I) at four temperatures. Each value of P^{-1} is the mean of at least 8 separate determinations; standard deviations were not greater than $\pm 5\%$ of the mean. The lines through the data and the values of the intercepts were determined by linear regression.
- Figure 2:** Interfacial transfer rate constants, k_{oa} (organic \rightarrow aqueous, panel [1]), and k_{ao} (aqueous \rightarrow organic, panel [2]) for methyl nicotinate as a function of (i) PEG concentration in the aqueous phase, and (ii) temperature. The values of the rate constants at 20°C, when PEG is absent, are from Albery et al.¹⁵
- Figure 3:** Enthalpic (ΔH_i^\ddagger) and entropic (ΔS_i^\ddagger) contributions to the free energy of activation at 25°C for interfacial transfer of methyl nicotinate (panel [1] organic \rightarrow aqueous; panel [2] aqueous \rightarrow organic) as a function of PEG concentration in the aqueous phase.

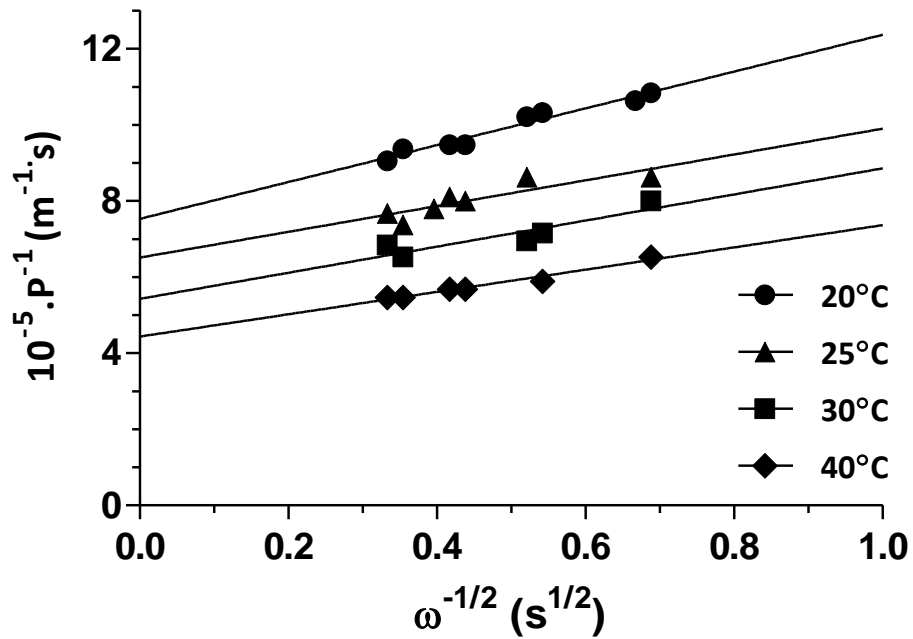


Figure 1: Dependence of total transport resistance (P^{-1}) on rotation speed ($\omega^{-1/2}$) for System B (see Table I) at four temperatures. Each value of P^{-1} is the mean of at least 8 separate determinations; standard deviations were not greater than $\pm 5\%$ of the mean. The lines through the data and the values of the intercepts were determined by linear regression.

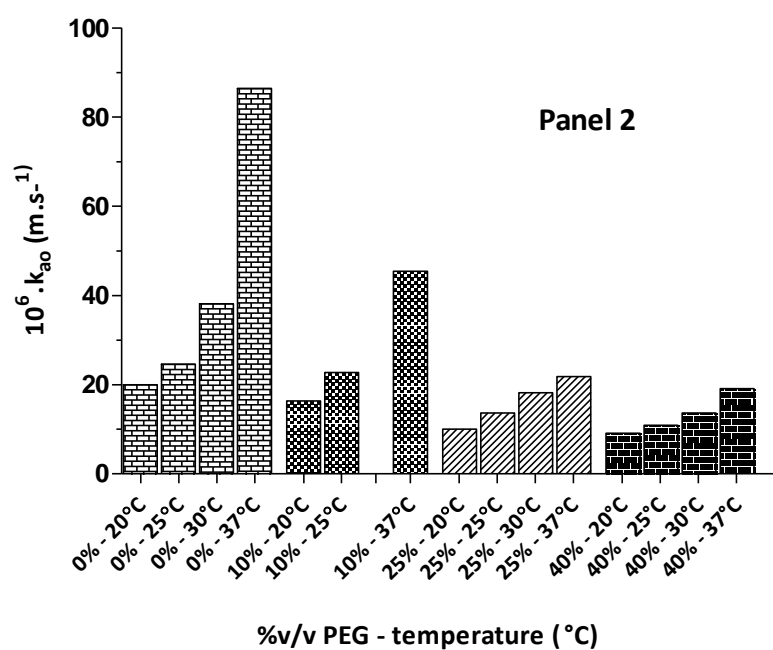
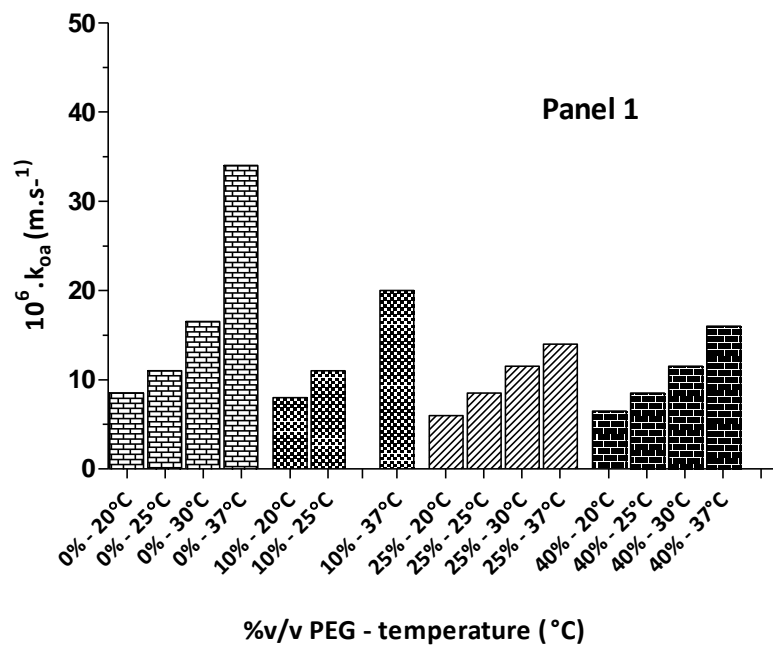


Figure 2: Interfacial transfer rate constants, k_{oa} (organic \rightarrow aqueous, panel [1]), and k_{ao} (aqueous \rightarrow organic, panel [2]) for methyl nicotinate as a function of (i) PEG concentration in the aqueous phase, and (ii) temperature. The values of the rate constants at 20°C, when PEG is absent, are from Albery et al.¹⁵

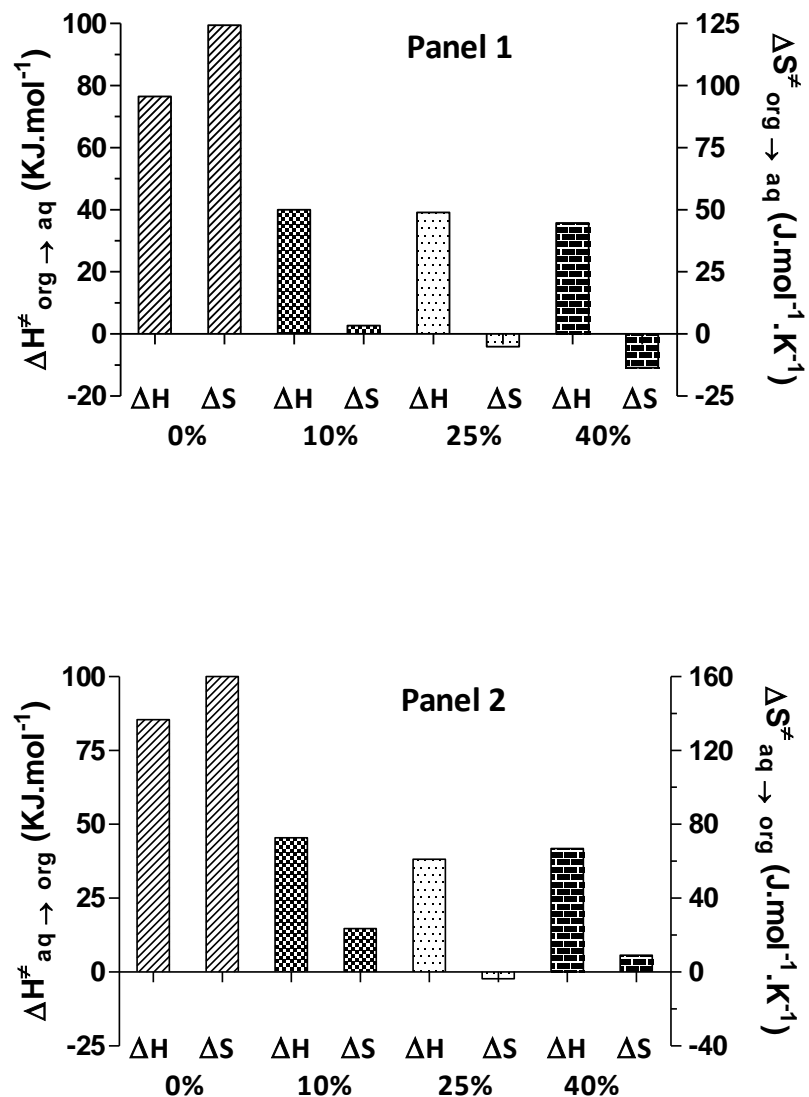


Figure 3: Enthalpic (ΔH_i^\ddagger) and entropic (ΔS_i^\ddagger) contributions to the free energy of activation at 25°C for interfacial transfer of methyl nicotinate (panel [1] organic \rightarrow aqueous; panel [2] aqueous \rightarrow organic) as a function of PEG concentration (% v/v) in the aqueous phase.